Arch. Metall. Mater. **64** (2019), 1, 365-369

DOI: 10.24425/amm.2019.126261

M. PETRIČ*, P. MRVAR*, S. KASTELIC*#

PREDICTION OF MICROSTRUCTURE OF GREY CAST IRONS BY ELECTRICAL RESISTIVITY MEASUREMENTS

The paper describes the influence of graphite shape, size and amount to electrical properties of different cast irons. Experiments of electrical resistivity measurements were conducted during solidification of four different melts in different time intervals from melt treatment by inoculation and nodularization. Metallographic analyses were made in order to determine the shape, size, distribution and amount of graphite and correlate results with electrical resistivity measurements. It was found out that nodular graphite is giving the lowest electrical resistivity and is decreased during solidification. Electrical resistivity of lamellar cast iron is increased during solidification since lamellas interrupt metal matrix severely There is no significant difference in resistivity of vermicular cast iron from nodular cast iron. Smaller size of graphite and lower amount of graphite and higher amount of metal matrix also decrease resistivity.

Keywords: Solidification, grey cast iron, electrical resistivity, graphite shape, microstructure

1. Introduction

Simple thermal analysis is well established method for solidification path monitoring of metals and alloys especially in aluminium and cast iron foundry industry. The results give us information of solidified microstructure in terms of phase fractions, shapes of microstructural constituents, presence of carbides, inclusions, etc. The measurement is based on heat release during solidification which is exothermal process. The heat release can be connected to individual phase or eutectic and in this way the microstructure can be predicted.

Electrical resistivity is a property of materials which is changed by temperature and it depends also on microstructure. [1,2].

In cast irons the microstructure usually first consists from austenite dendrites and eutectic graphite which can be lamellar, nodular etc. Austenite is later transformed to pearlite and/or ferrite. The involved phases and amounts of phases and the shape of phases have big influence on electrical resistivity of material. It is reported that shape and size of present phases has important influence on the electrical resistivity of material. If the phases are large and acicular or lamellar the electrical resistivity is higher because there are more interfaces – barriers for electrons to overcome. On the other hand, if phases are smaller and more rounded the electrical resistivity is lower [3,4].

There is no difference at cast irons. Very few reports have been found in literature. Stefanescu et al. [5] reported that electrical resistivity of lamellar grey cast irons is higher than the one of nodular cast irons. There is also stated that the matrix also influences the electrical resistivity and it is higher if it is pearlitic than ferritic [6].

The aim of the study is to investigate the influence of graphite shape and size, the amount of graphite and the influence of chemical composition to electrical resistivity of different cast irons; lamellar, vermicular and nodular respectively.

2. Experimental

In the study different melts of lamellar and nodular cast iron were prepared and tested by electrical resistivity measurements. We prepared two lamellar cast iron melts (L1 and L2) and two nodular cast iron melts (N1 and N2) with chemical compositions given in Table 1. They have similar carbon equivalents (CE), but there are differences in carbon (C) content and titanium (Ti) and silicon (Si) contents for lamellar cast iron melts. Charge materials of approximately 6 kg were melted in an induction furnace in graphite crucible. After remelting the melts were inoculated and in the cases of nodular cast iron also Mg treated by agents with compositions given in Table 2. Additions of inoculant for lamellar cast irons were 0,2 wt. %. In a sample L1 we additionally added some pure Ti to increase its level to 0,034 wt. %. At production of nodular cast iron, the procedure was similar where the plunging method was used for introduction of nodularizer and inoculant in amounts of 1 wt. % and 0,2 wt.% respectively. After treatment of each melt three samples were cast into measuring cells described hereinafter. Samples were taken at different times after melt treatment in order to investigate the influence of fad-

* UNIVERSITY OF LJUBLJANA, FACULTY OF NATURAL SCIENCES AND ENGINEERING, LJUBLJANA, SLOVENIA

Corresponding author: sebastjan.kastelic@omm.ntf.uni-lj.si

ing effect to microstructure which results at electrical properties during solidification. The times of sampling were each 15 min for samples L1, L2 and N2 and each 5 min for sample N1. All together twelve samples were taken.

TABLE 1

Chemical compositions of investigated melts

Samples	Chemical composition (wt. %)							
	C	Si	P	Mn	S	Mg	Ti	CE
L1	3.51	2.16	0.012	0.45	0.052	0.001	0.034	**4.23**
L2	3.25	1.76	0.035	0.51	0.040	0.001	0.09	**3.83**
N1	3.29	2.51	0.022	0.225	0.013	0.068	0.011	**4.12**
N2	3.40	2.53	0.022	0.226	0.013	0.079	0.010	**4.21**

TABLE 2

Chemical compositions of inoculants and nodularizer

	Chemical composition (wt. %)							
	Fe	Si	Ca	Al	Ba	Mg	Ti	RE
Inoculant (L1, L2)	Rest	50-55	0.5-1.5	—	—	—	9-11	—
Nodularizer (N1, N2)	Rest	44-48	0.8-1.2	0.4-1.0	—	5.5-6.2		0.8-1.2
Inoculant (N1, N2)	Rest	64-70	1.0-2.0	0.8-1.5	2.0-3.0	—		—

The four-probe DC technique was used for measuring electrical resistivity during solidification as thoroughly described in previous work [7] where low carbon steel wires with diameter of 1,6 mm were used as electrodes. Simultaneously the thermal analysis was carried out by K-type thermocouple positioned under the sprue. All the data were captured by National Instruments CompactDAQ NI 9213 and NI 9219 measuring cards.

Acquired data was then plotted in form of curves presenting electrical resistivity vs. temperature and/or time. Electrical resistivity (ρ) was calculated according to Eq. (1):

$$\rho = R\frac{S}{l} \tag{1}$$

where R is measured resistance, S and l are cross-section and measured length of a sample (170 mm). Cooling curves representing solidification path were plotted as well.

All samples were metallographically examined in order to determine the shape of graphite, size, distribution, amount of graphite and the matrix. Metallographic observations were done by Olympus BX 61 optic microscope in polished state. The size and shape of graphite was determined automatically by Analysis 5.0 software.

3. Results and discussion

3.1. Metallographic analyses

Metallographic observations of all samples were done on the cross-sections of the cast sample taken just next to the sprue as presented on Fig. 1. At least five microphotographs were taken from one sample for statistical analyses of microstructure. The measured data for all four samples are summarized in a Table 3 where the time of sampling after melt treatment is given for each sample, CE, amount of graphite and the size of graphite. In the case of lamellar cast irons, the distribution of graphite is given and at nodular cast irons the shape of graphite is given. All parameters are determined according to EN ISO 945 standard.

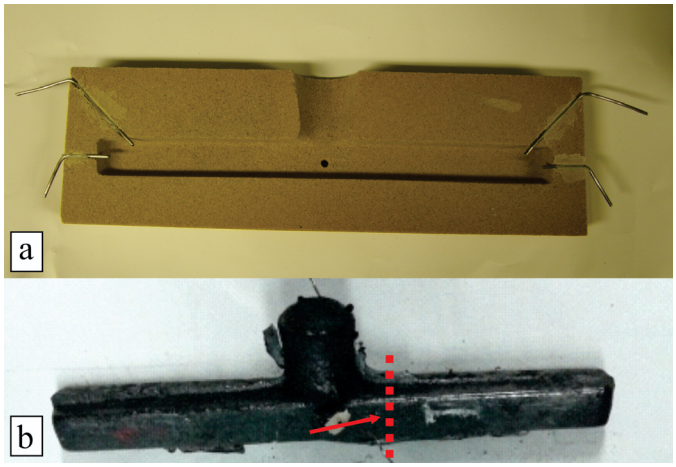

Fig. 1. Measuring cell (a) and a cast sample with marked position of metallographic observations

TABLE 3

A list of samples with time delays of sampling, CE, distribution and shape of graphite, amount and size of graphite according to EN ISO 945 standard

Sample	Specimen	Time/ min	CE	Distribution / Shape	Gr/%	Size
L1	**L1-0**	0	4,23	80% I A 6 + 20% I D	14,1	6
	L1-15	15	4,04	A, D(25 %)	10,9	6
	L1-30	30	3,95	D(100 %)	6	7
L2	**L2-0**	0	3,83	A, D(32 %)	9,8	6
	L2-15	15	3,74	A, D(85 %)	9,8	6,6
	L2-30	30	3,67	D(100 %)	6,8	7
N1	**N1-0**	0	4,32	VI	6,0	7
	N1-5	5	4,26	V, III(35 %)	5,8	6
	N1-10	10	4,26	I, III(35 %)	5,0	6
N2	**N2-0**	0	4,21	VI	4,8	7
	N2-15	15	4,47	I, III(30 %)	3,7	6
	N2-30	30	4,40	III, II(45 %)	7,7	8

It has been recognized that CE is decreased with holding time because of the carbon burnout. There is one deviation from this statement at sample N1-15 where CE is increased. The reason for this was the use of new melting crucible where carbon was diffusing from the crucible into the melt. It is well established that the time after melt treatment has negative results for graphite shape and distribution and this is confirmed here as well. One can see that the distribution of graphite in lamellar cast irons is mainly from class A for first samples and is changed to the

class D in samples taken 30 min after melt treatment. Similar result is observed at nodular cast irons where in first sample the graphite shape is from class VI which is nodular and is more and more transformed into class III and I which are vermicular and lamellar respectively. This is again a consequence of Mg burnout. The amount of graphite is changed during the time as well in accordance with CE but there are some deviations as well probably because randomly taken microphotographs and, in some cases, small graphite particles which are difficult to detect at image analyses. In a case of N2-30 sample this analysis of amount of graphite and also the shape of graphite is not representative.

Fig. 2 is presenting representative microphotographs of all twelve samples where graphite shape and distribution can be seen. All four melts have in common that with time the distribution of graphite is deteriorating, and the sphericity of graphite nodules is reduced, and more and more vermicular graphite appears. In samples L1-0 and L2-0 the graphite distribution is mainly class A and also some undercooled graphite from class D. With longer holding time the amount of D class graphite increases and after 30 min only D remains. The metallographic observations are also revealing dendritic structure which quantity is increased with holding time.

At nodular cast irons the fading effect of Mg treatment is visible already after 5 min holding time where vermicular graphite is already appearing (N1-5 in Fig. 2). After 15 min the microstructure is mainly from vermicular graphite and microstructure is inhomogeneous where larger areas of iron matrix appear. 30 min after Mg treatment lamellar graphite in very small sized lamellas is formed in N2-30 sample.

3.2. Electrical resistivity measurements

Figs. 3 and 4 are presenting curves of measured electrical resistivity vs. temperature. As it is already written above the electrical resistivity curve of lamellar cast iron is different than

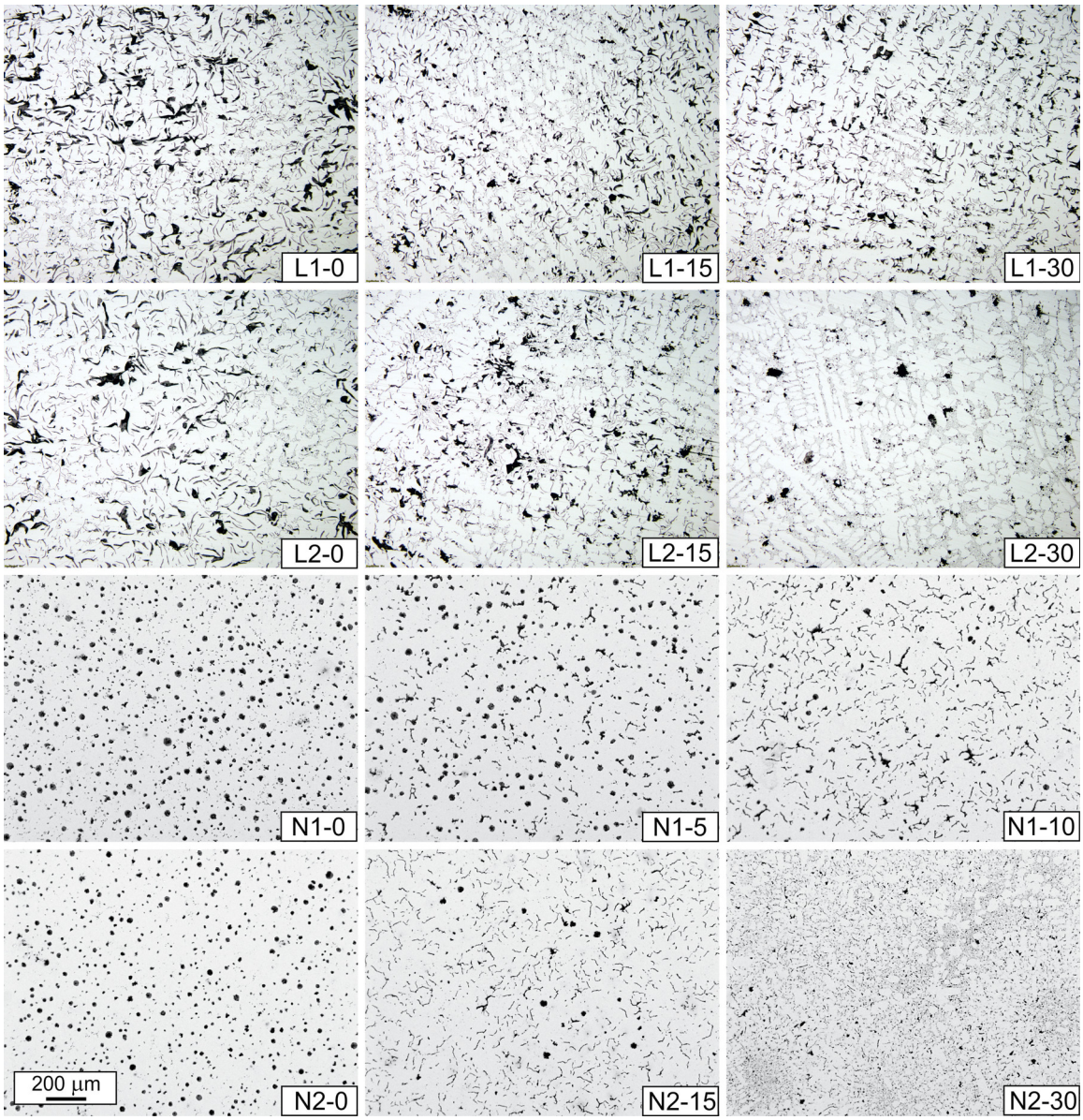

Fig. 2. Microstructures of all samples

it is expected at pure metals. It is seen that it is also the case for melts L1 and L2 (Fig. 3) since they have lamellar graphite and the resistivity is increased during solidification. At each Fig. for melt L1 and L2 three curves are presented where each of the curve represents samples with delayed pouring time. From these results it is clear that the holding time from melt treatment to pouring has an influence on electrical resistivity. The electrical resistivity after solidification is decreased with longer time. The reason for this can be found in Fig. 2 where one can see the size and distribution of graphite. Smaller lamellas mean lower electrical resistivity as it was already reported for other alloys or composites [3,4]. At samples with the longest holding time the distribution of graphite is from class D where large amount of matrix or dendrites is present. Metallic matrix has better conductivity than the eutectic, so it means that the electrons are less scattered when traveling through metallic matrix and consequently the electrical resistivity is lower. As presented in Table 3 the CE and the amount of graphite are also changed with time which in lesser amounts also cause a decrease in electrical resistivity. However, the electrical resistivity of melt prior to solidification is approximately the same for each melt, the deviations are most probably caused by slightly changed cross-sections of cast samples since the measuring cells are manually produced.

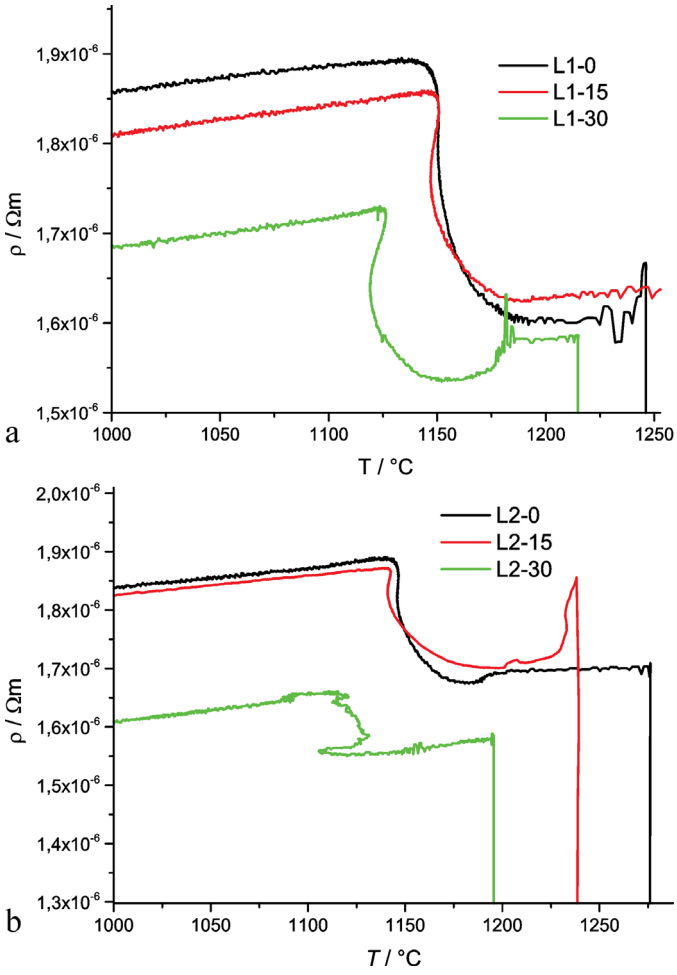

Fig. 3. Electrical resistivity curves vs. temperature for melt L1 (a) and melt L2 (b)

Fig. 4 is presenting electrical resistivity curves of malts N1 and N2. From samples N1 (Fig. 4a) it is seen that all three curves are decreased during solidification which is expected for nodular cast irons where nodules do not interrupt the matrix so severely. From Fig. 2 it is also seen that with holding time the shape of nodular graphite is degenerated towards vermicular graphite which should increase electrical resistivity and it surely does. But in the same time also the CE and the amount and the size of graphite are decreased (Table 3) and they have opposite effect, so the described phenomena is not detected.

Very similar situation is recorded at the samples from the melt N2 (Fig. 4b). With increased holding time the electrical resistivity during and after solidification is decreased even if the shape of graphite is becoming vermicular. Same effect as in melt L1 is present. In the last taken sample (L2-30) the curve changes its shape into a lamellar one since Mg content is too low and the lamellar graphite appears.

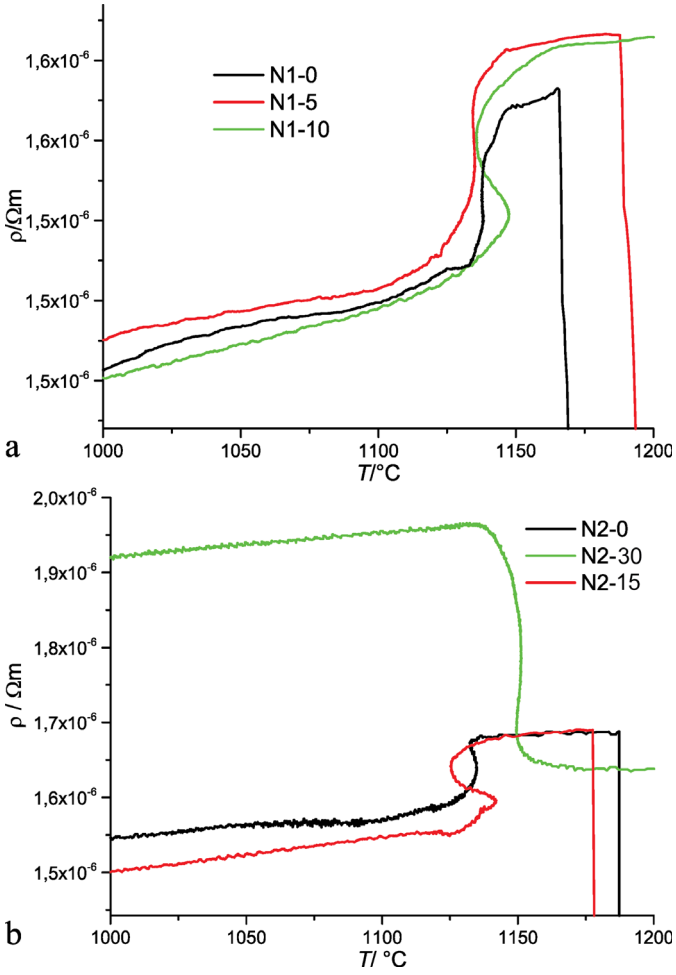

Fig. 4. Electrical resistivity curves vs. temperature for melt N1 (a) and melt N2 (b)

4. Conclusion

A presented research is dealing with prediction of microstructure in particularly graphite shape for different cast irons by electrical resistivity measurements during solidification. Samples

were taken from treated melt in different time intervals to see the fading effect of inoculation and Mg treatment which results in degenerated shape of graphite and distribution.

In lamellar melts it was observed that the electrical resistivity during solidification is increased. With longer holding times the inoculation of melt faded so the size of graphite particles was lowered, and the amount of graphite was decreased which as well caused a decrease of electrical resistivity after solidification in comparison with well inoculated melt. Additionally, faded inoculation resulted in D type graphite and appearance of dendritic structure which gives lower electrical resistivity.

At nodular cast iron melts, the electrical resistivity was decreased during solidification since the nodules do not interrupt a conducting matrix so much as lamellas. Although a holding time had negative effect for sphericity of graphite and vermicular graphite appeared. It was expected that the electrical resistivity would be increased during solidification, but the lowered CE and decreased amount of graphite compensated the influence of graphite shape change and the phenomena of increased resistivity was not seen.

For fully understanding of electrical resistivity curves recorded during solidification and corelating them with graphite shape additional experiments will be needed. The tested melts will have to have controlled chemical compositions resulting in graphite shape, size and amount. Only in this way the recorded curves will be comparable and representative.

Acknowledgements

The author would like to acknowledge foundries Livar d.d. and Omco Metals d.o.o. for enabling and support this research.

REFERENCES

[1] A.R. Sinigoj, Basics of Electromagnetics, Publisher of Faculty of Electrical engineering and Faculty for Computer and Information Science (in Slovenian), Ljubljana (1999).

[2] T.E. Faber, An introduction to the theory of liquid metals, Cambridge University Press, New York (1972).

[3] L. Weber, C. Fischer, A. Mortensen, On the influence of the shape of randomly oriented, non-conducting inclusions in a conducting matrix on the effective electrical conductivity, Acta Materialia **51**, 495-505 (2003).

[4] L. Weber, J. Dorn, A. Mortensen, On the electrical conductivity of metal matrix composites containing high volume fractions of non-conducting inclusions, Acta Materialia **51**, 3199-3211 (2003).

[5] D.M. Stefanescu, S.T. Craciun, Bestimmung der graphitform im gusseisen durch messung des spzifischen elektrischen widerstandes waehrend der erstarrung, Giesserei-praxis **11**, 197-200 (1973).

[6] D.M. Stefanescu, H. Weingert, Einfluss des graphits und der metallischen grundmasse auf den spezifischen elektrischen widerstand von gusseisen mit lamellen-bzw. Kugelgraphit, Giesserei-praxis **14**, 256-261 (1971).

[7] M. Petrič, S. Kastelic, P. Mrvar, Selection of electrodes for "in situ" electrical resistivity measurements of molten aluminium, Journal of Mining and Metallurgy – Section B-Metallurgy **49** (3), 279-283 (2013).